Practical of NanoScience

Static and Dynamic Light Scattering

written by:

Katharina Wingert

Supervisor

PD Dr. Fajun Zhang

C07H09

AG. Prof. Dr. Frank Schreiber

Institute of Applied Physics

Eberhard-Karls-Universität Tübingen

Oct. 2012, revision 2018

Contents

1 Safety Issue

Before using a laser it is important to be informed about the potential dangers. Students will be informed for the laser protection. One can also find a document called *"Was man im Umgang mit Lasern beachten muß"'* on the 'F-Praktikums-'Website.

For the experimental procedure a laser with a hazard class 1 is used with a continuous output of 22mW. In practice, the apparatus has a safety cover which blocks all possible exposure of laser. Laser pointers (red and green) are assigned to laser class 2 which send out visible radiation within a wavelength range from 400nm to 700 nm. It is dangerous for the eye at a dwell time above 0.25 sec (eye lid reflex).

2 Introduction

Scattering techniques including light, X-ray and neutron scattering have been widely used in Biology, Chemistry, Physics, material science as well as many other research fields. They are powerful analytical tools providing structural information in a length-scale range from Angstrom to micrometer and collective dynamics from the picosecond up to millisecond range. This practical is designed as an introduction for students with basic principles of scattering technique in general. The light scattering setup provides the basic components needed for almost any scattering technique. The selected experiments are used to demonstrate (what) structural and dynamic information one can get from a static and dynamic light scattering measurement.

In 1868, the Irish physicist John Tyndall was the first to examine light scattering of colloidal solutions. He noticed that a white light beam which passes through a gold colloidal dispersion (sol) is visible from the side. He could observe blue scattered light perpendicular to the incident light beam. This phenomenon depends on the type, size and shape of the particles and on the wavelength of the scattered light. The relationship between the sizes of the particles compared to the wavelength of the incident light beam shows a differentiation between scattering at large particles with $d>\lambda/20$ and scattering at small particles with $d<\lambda/20$. In 1871 Lord Rayleigh was able to describe the light scattering in theory which explains also the blue color of a cloudless sky.

Nowadays light scattering is a very powerful method to characterize the structure, dynamics and mass of polymers and nanoparticles in solutions. For this purpose, a laser beam with a defined wavelength λ is guide to a (dissolved) sample, usually in solution. The scattered intensity is then measured at various scattering angles by a detector.
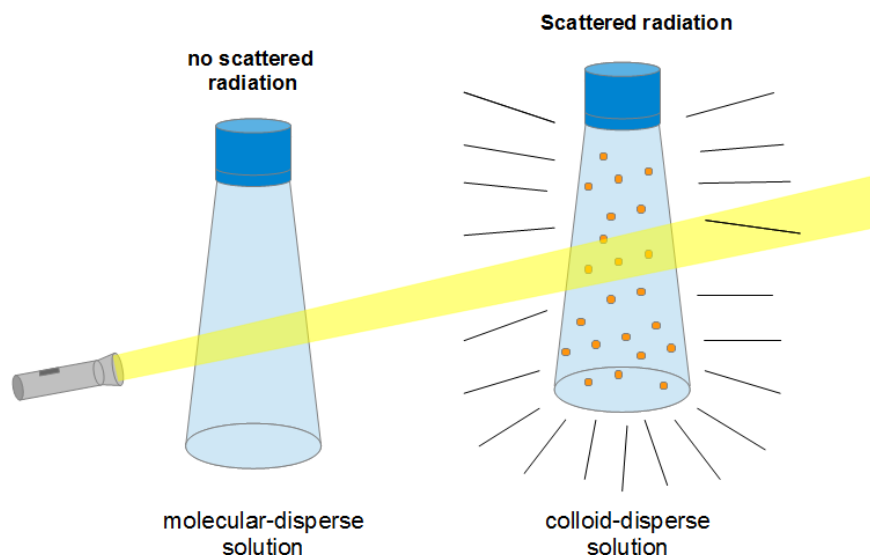
Figure 1: Schematic representation of the Tyndall effect.

As the name implies static light scattering (SLS) focuses on the static behavior. Only the averaged intensity is recorded as a function of scattering angle, which is used to determine the average molecular weight, the second virial coefficient and the radius of gyration of the particles. In dynamic light scattering (DLS), one examines the diffusion of the particles by recording the intensity as a function of time which is used to determine the diffusion coefficient and the hydrodynamic radius.

Note for practical in NanoScience, we focus on the application of dynamic light scattering in bio- and nano-systems. However, the theoretical part on static light scattering is important for understanding the angular dependent scattering.

3 Basic Principles of Light Scattering

3.1 Static Light Scattering (SLS)

3.1.1 Interactions of light with matter

Light scattering means that an incident electromagnetic wave is deflected by the interaction with a molecule from its original direction of propagation to another. The theory is that the incident electromagnetic wave induces in the atomic shell electric dipoles.

These oscillating dipoles act as emitters of electromagnetic waves of the same wavelength as the incident one but with different propagation directions. The angle between the incoming and scattering wave is called scattering angle Θ.
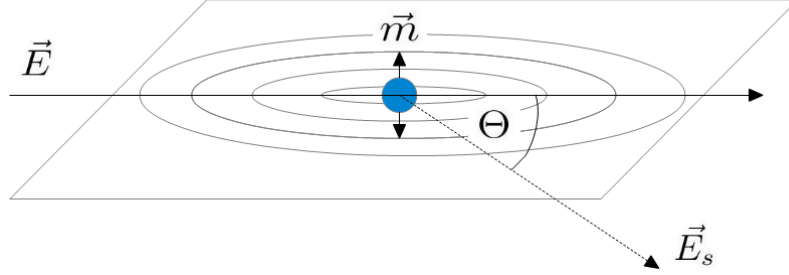

Figure 2: Induction of an oscillating dipole caused by an incoming electromagnetic wave

With the scattering angle Θ, the wavelength of the incident beam λ and the refractive index of the solvent n_{LM} we can define the scattering vector $\vec{q}$, which is the difference between the incoming $\vec{k_0}$ and outcoming beam $\vec{k}$ ($\vec{q} = \vec{k_0} - \vec{k}$) with the unit $[\mathrm{m}^{-1}]$ and $\left|\vec{k}\right| = \left|\vec{k_0}\right| = 2\pi/\lambda$ as
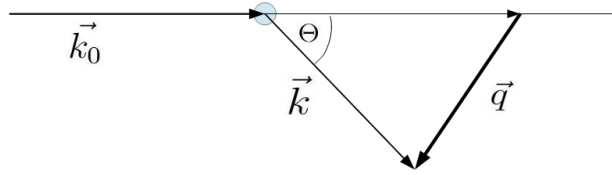

Figure 3: Sketch of the definition of the scattering vector $\vec{q}$.

$$q = \frac{4\pi n_{\mathrm{SV}}}{\lambda} \sin\left(\frac{\Theta}{2}\right) \tag{1}$$

For particles with a diameter smaller than $\lambda/20$ only a negligible phase difference exists between light emitted from the various scattering centers within the given particle. In this case the detected scattered intensity will be independent of the scattering angle (see Fig. 4). The elastic scattering process (incoming and scattered electromagnetic waves have the same wavelength) is called *Rayleigh-Scattering*. But for molecules or particles with a diameter larger than $\lambda/20$, some of these simultaneously created dipoles emit light waves with a significant phase difference. This leads to a nonisotropic angular dependence on the scattered light intensity. These intermolecular interferences result in

the so called angle depending particle form factor $P(q)$, informing about shape and size of the scattered particles.
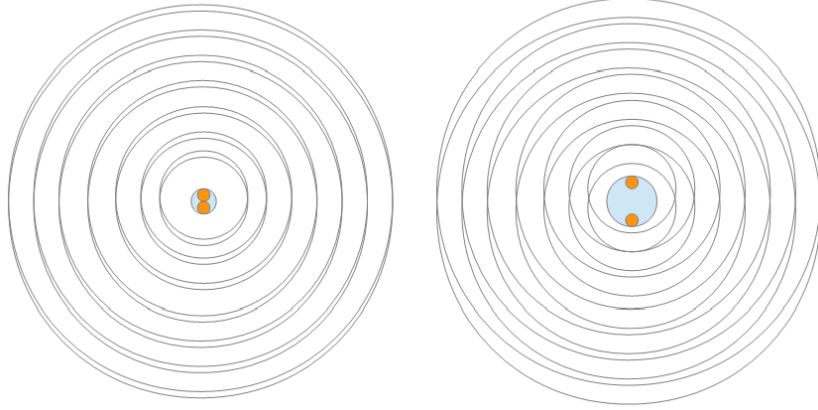

Figure 4: Interference pattern of light scattered from small particles (left) and from larger particles (right) illustrated with two scattering centers.

As mentioned above, matter scatters electromagnetic waves due to the induction of an oscillating electric dipole as shown in Fig. 2. This dipole serves as a source for the scattered light wave. The electric dipole momentum $\vec{m}$ depends on the polarizability α of the excited medium and the electric field vector $\vec{E}$ of the incident electromagnetic wave as:

$$\vec{m} = \alpha \vec{E} \tag{2}$$

$\nu = \frac{c}{\lambda}$ describes the frequency of the lightbeam with a wavelength λ and $k = \frac{2\pi}{\lambda}$ the length of the wave vector. The electric field vectorof the scattered beam E_s the following equation is given by

$$E_\mathrm{s} = \left(\frac{\partial^2 m}{\partial t^2} \right) \frac{1}{r_\mathrm{D} c_0^2} = \frac{-4\pi^2 \nu^2 \alpha E_0}{r_\mathrm{D} c^2} e^{i(2\pi\nu t - \vec{k}\vec{r}_\mathrm{D})} \tag{3}$$

$\vec{r}_\mathrm{D}$ describes the distance vector from the scattering sample to the detector, c_0 the speed of light and E_0 the electric field of the incident beam. In a typical light scattering experiment only the scattered intensity $I_\mathrm{s} = E_\mathrm{s} \cdot E_\mathrm{s}^* = |E_\mathrm{s}|^2$ is detected, but not the

amplitude of the corresponding electric field. The basic setup for a light scattering experiment is illustrated in Fig. 5.
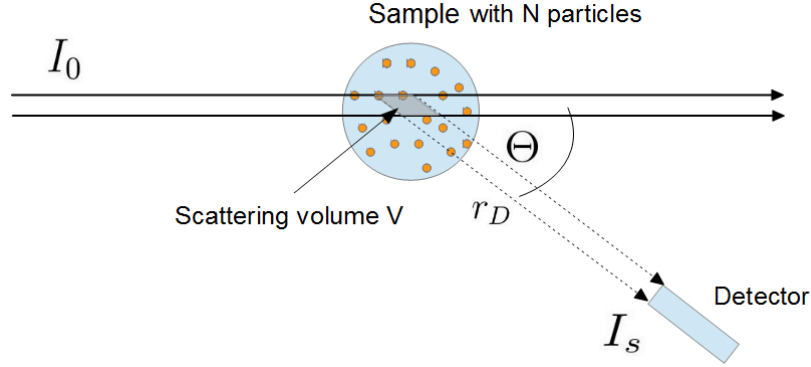

Figure 5: Schematic construction of a light scattering apparatus.

I_0 is the intensity of the incident light beam, I_s the intensity of the scattered light.

Assuming that the scattered particles move randomly in space and that they are very small and therefore can be considered as a point scatterer, Rayleigh discovered a relationship between the intensity of the primary light I_0 and the scattered light I_s according to Maxwell theory of electrodynamics:

$$I_s = I_0 \cdot \frac{V}{r_D^2} \frac{16\pi^4}{\lambda^4} \alpha^2 \cdot \varrho \tag{4}$$

It the case the relationship applies only by using vertically polarized light. Abbreviations:

r_D	Distance between scattering center and detector
V	detected scattering volume (see Fig. 5)
α^2	Square of the polarizability
λ	Wavelength of light in vacuum
$\varrho = \frac{N}{V}$	Number of scattering particles per volume

As shown in Eq. 4 the scattered intensity scales inversely with the forth power of the wavelength of the incident light. (This is the reason why the sky is blue because the shorter wavelength blue light scatters more intensively than the other wavelengths

of visible light.) It turns out that in particular the polarizability α plays a crucial role in scattering theory. In order to separate the setup dependent from the setup independent variables in Eq. 4 we can rewrite the equation as follows:

$$R \equiv I_{\mathrm{s}} \cdot \underbrace{\frac{1}{I_0} \cdot \frac{r_{\mathrm{D}}^2}{V}}_{\text{apparatus factor}} = \frac{16\pi^4}{\lambda^4} \alpha^2 \cdot \varrho \tag{5}$$

Here the incident wavelength was counted to the setup independent variable because this can easily reproduce in other setups by using a light source with the correct wavelength. The setup dependent part is defined by the Rayleigh ratio R. In practice, the Rayleigh ratio R can be determined by measuring a standard sample like toluene. From this standard sample the absolute scattering intensity $I_{std,absolute}$ is known in literature, e. g. for toluene this absolute scattering intensity is $I_{Std,abs} = 1.39 \cdot 10^{-5}\,\mathrm{cm}^{-1}$ for a wavelength of 632.8 nm and a temperature of 20°C. By dividing the $I_{std,absolute}$ by the measured scattering intensity from the used standard I_{std} the scattering intensity from real samples can be scaled to absolute intensities. This procedure can be described by the following equation for the Rayleigh ratio.


Figure 6: Measured Rayleigh ratio.

3.1.2 Rayleigh-Scattering ($d < \lambda/20$)

In the following section we will consider the scattering of dilute solutions of small particles. In this case the detected scattered intensity is independent from the scattering angle Θ. The number density of such system can be described by the following equations

$$N = \frac{cVN_\mathrm{A}}{M} \iff \varrho = \frac{N}{V} = \frac{cN_\mathrm{A}}{M} \tag{6}$$

where c is concentration , V the scattering volume, M the molar mass of a particle and N_A the Avogadro constant. According to the Clausius-Mossotti equation the polarizability α can be replaced by the refraction index of the solution n_SL and of the solvent n_SV as follows (SL is standing for 'solution' and SV for 'solvent'):

$$\alpha \equiv \frac{n_\mathrm{SL}^2 - n_\mathrm{SV}^2}{4\pi\varrho} \stackrel{(6)}{=} \frac{M(n_\mathrm{SL}^2 - n_\mathrm{SV}^2)}{4\pi c N_\mathrm{A}} \tag{7}$$

With the following approximation $\frac{n_\mathrm{SL}^2 - n_\mathrm{SV}^2}{c} \approx 2n_\mathrm{SV}\left(\frac{\partial n_\mathrm{SL}}{\partial c}\right)$ Eq. 4 can be transformed with Eq. 7 and Eq. 6 as:

$$I_\mathrm{s} = \underbrace{I_0 \cdot \frac{V}{r_\mathrm{D}^2}}_{\text{apparatus constant}} \cdot \underbrace{\frac{4\pi^2}{\lambda^4 N_\mathrm{A}} \cdot n_\mathrm{SV}^2 \left(\frac{\partial n_\mathrm{SL}}{\partial c}\right)^2 \cdot cM}_{\text{contrast factor } K := b^2} \propto K \cdot cM \tag{8}$$

The middle term is called contrast factor K or rather square of the scattering power b with unit of $\left[\frac{\mathrm{cm}^2\mathrm{mol}}{\mathrm{g}^2}\right]$.

The refractive index increment $\frac{\partial n_\mathrm{SL}}{\partial c}$ of Eq. 8 describes the change of the refractive index with changing concentration. The refractive index increment is measurable with a differential refractometer. For standard samples, the ratio $\frac{\partial n_\mathrm{SL}}{\partial c}$ can be found in literature or handbooks. Note that this value depends on the temperature T of the solution, the wavelength λ of the incident light beam and the solvent in which the particles are dissolved.

Combining Eq. 5 and Eq. 8, one has

$$R = b^2 \cdot cM = \frac{4\pi^2}{\lambda^4} n_\mathrm{SV}^2 \left(\frac{\partial n_\mathrm{SL}}{\partial c}\right)^2 \frac{cM}{N_\mathrm{A}} \tag{9}$$

$$\stackrel{(x)}{=} (I_\mathrm{SL} - I_\mathrm{SV}) \underbrace{\frac{r_\mathrm{D}^2}{V}}_{*} \tag{10}$$

Step (x) profits from the fact that the absolute scattering intensity I_SAMPLE is composed by the difference of I_SL and I_SV.

Eq. 8 describes the scattering intensity from an ideal solution, in which any intermolecular interference can be neglected. In real systems, the scattering intensity I_s is dependent on the scattering power b (with $b^2 = K$) and the osmotic pressure. Both the scattering vector as well as the osmotic pressure are dependent on changes of the concentration.

$$I_s \propto b^2 \mathrm{R} T \frac{c}{(\frac{\partial \pi}{\partial c})_{\mathrm{T,N}}} \tag{11}$$

k corresponds to the gas constant $k = N_A k_B$.

According to van't Hoff the partial derivative of the osmotic pressure with respect to the concentration is:

$$
\begin{aligned}
\frac{\partial \pi}{\partial c} &= \frac{kT}{M} & \text{(ideal solution)} \tag{12}\\
\frac{\partial \pi}{\partial c} &= kT(\frac{1}{M} + 2A_2 c + ...) & \text{(real solution)} \tag{13}
\end{aligned}
$$

where M is the molecular weight and A_2 the second viral coefficient which provides a quantitative measure for the interactions between solute molecules. $A_2 = 0$ indicates the effective interactions between solute molecules is zero. $A_2 < 0$ indicates that the overall interactions between particles are attractive; $A_2 > 0$ indicates that the overall interactions are repulsive.

Altogether Eq. 11 can be transformed to:

$$\boxed{\frac{Kc}{R} = \frac{1}{M} + 2A_2 c + ...} \tag{14}$$

With the Rayleigh-Ratio R of Fig. 6. In Experiment $\frac{Kc}{R}$ is specified directly. This corresponds to an inverse already normalized intensity which matches the experimental apparatus and the solvent.

3.1.3 SLS of larger particles ($d > \lambda/20$)

For particles with a diameter of $d > \lambda/20$, the interference of the scattered light from different scattering centers cannot be neglected, as pictured in Figure 7. Therefore, the scattered light intensity shows an angle dependent pattern.
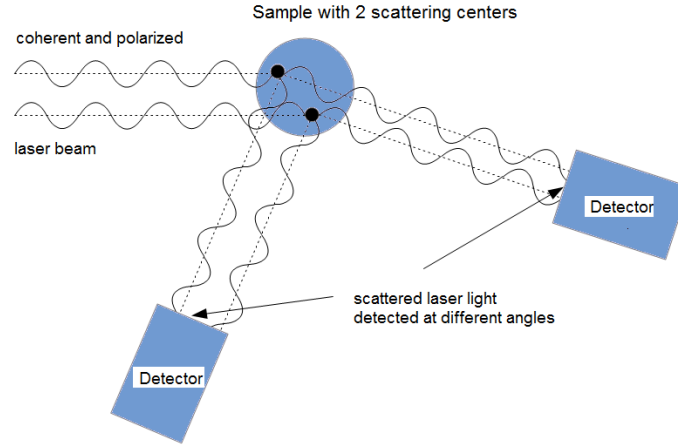
Figure 7: Schematic representation of light scattering from two scattering centers in a large particle. Depending on the scattering angle at which the intensity is detected, different interferences of the scattered radiation occur.

This angle dependent scattering pattern of an individual particle is called form factor $P(q)$.

The following section explains how the particle form factor $P(q)$ is derived. For two scattering centers in a particle with the distance vector $\vec{r}_{ij}$ can be shown that the phase shift φ of the outgoing light waves can be described as $\varphi = -\vec{q}\vec{r}$, which varies as a function of the scattering angle Θ or rather $\vec{q}$. For a sample of N identical particles within the scattering volume, each particle containing Z scattering centers, the scattered intensity $I(q)$ is obtained by pairwise summation over all scattering centers:

$$I(q) = N^2 b^2 \left| \left\langle \sum_{i=1}^{Z} \sum_{j=1}^{Z} e^{-i\vec{q}\vec{r}_{ij}} \right\rangle \right| \tag{15}$$

where $\vec{r}_{ij} = \vec{r}_i - \vec{r}_j$. For very dilute solutions so that the interferences between different scattering particles can be neglected. The detected intensity $I(q)$ is only caused by intraparticular interferences. By normalizing the scattered intensity using the number of particles, we obtain the following particle form factor $P(q)$:

$$P(q) \quad = \quad \frac{1}{N^2 Z^2 b^2} I(q) = \frac{1}{Z^2} \left| \left\langle \sum_{i=1}^{Z} \sum_{j=1}^{Z} e^{-i\vec{q}\vec{r}_{ij}} \right\rangle \right| = \frac{1}{Z^2} \left\langle \sum_{i=1}^{Z} \sum_{j=1}^{Z} \left(\frac{\sin q r_{ij}}{q r_{ij}} \right) \right\rangle \quad (16)$$

$$= \quad \frac{1}{Z^2} \sum_{i=1}^{Z} \left\langle \sum_{j=1}^{Z} \left(1 - \frac{1}{6} q^2 r_{ij}^2 + ... \right) \right\rangle \quad (17)$$

Radius of gyration Using the center of mass coordinate system, as shown in Fig. 8. Instead of using cartesian coordinates $\vec{r}_j$, the center of mass-based position vectors $\vec{s}_j$ can be used to simplify Eq. 17.
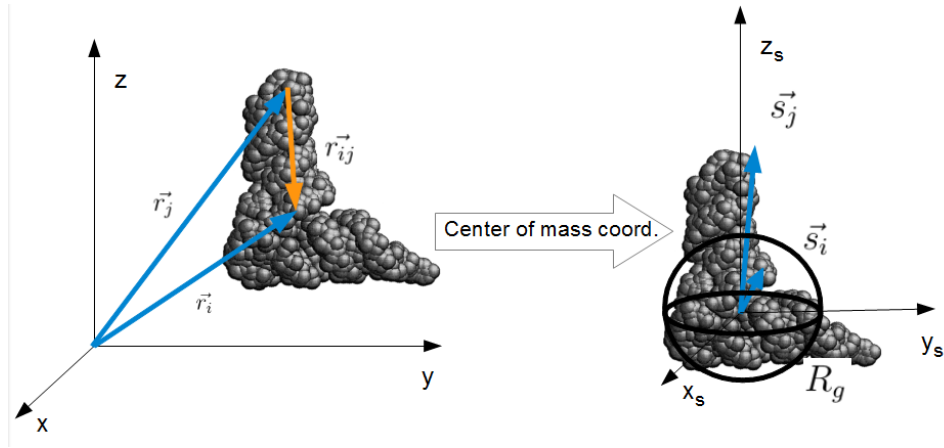

Figure 8: Transformation to center of mass coordinates.

Assuming a homogeneous particle with constant particle density, it is imperative:

$$\sum_{i=1}^{Z} \vec{s}_i = 0 \quad \text{and} \quad R_g^2 = \frac{1}{Z} \sum_{i=1}^{Z} \vec{s}_i^2 \neq 0 \quad (18)$$

$$\Longrightarrow ... \Longrightarrow \frac{1}{Z^2} \sum_{i=1}^{Z} \sum_{j=1}^{Z} r_{ij}^2 = 2R_g^2 \quad (19)$$

R_g describes the radius of gyration. Eq. 19 shows that the radius of gyration R_g is defined by the average distance from the scattering centers to the center of mass. For $qR < 1$ (particles with a radius between $10\,\text{nm} < r < 50\,\text{nm}$) the form factor of Eq. 17 can be approximated with the radius of gyration (Eq. 19) to:

$$P(q) = 1 - \frac{1}{3} \left\langle R_{\mathrm{g}}^2 \right\rangle q^2 \tag{20}$$

This relation is called the *Guinier-Approximation*. The inverse form of $P(q)$ can be written as $\frac{1}{P(q)} = 1 + \frac{1}{3} R_{\mathrm{g}}^2 q^2$ (recall Eq. 14). Now we have the so-called Zimm equation:

$$\boxed{\frac{Kc}{R} = \frac{1}{MP(q)} + 2A_2c + ... = \frac{1}{M}(1 + \frac{1}{3} \left\langle R_{\mathrm{g}}^2 \right\rangle q^2) + 2A_2c} \tag{21}$$
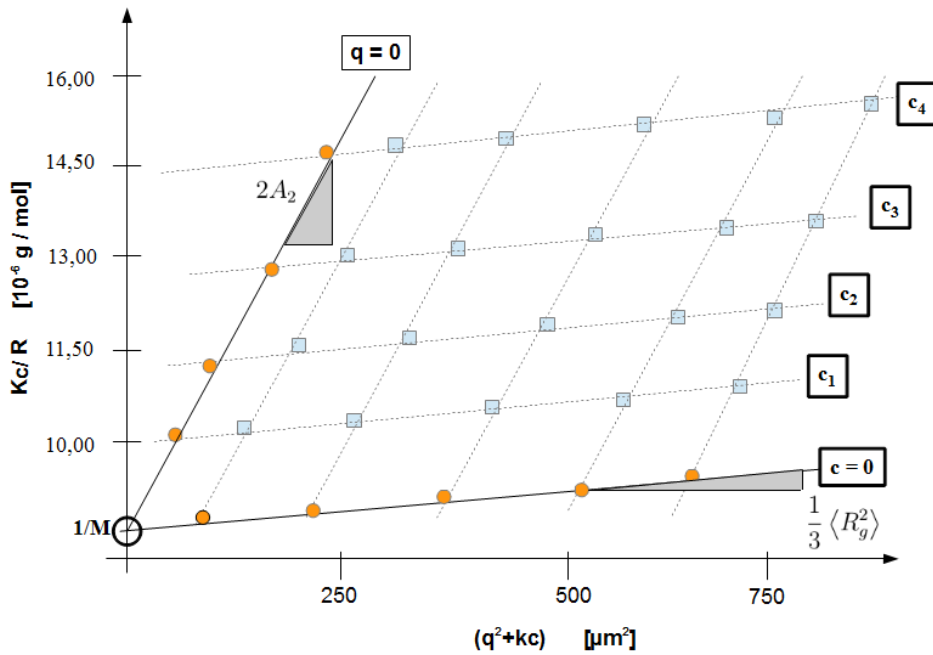

Figure 9: The Zimm plot is obtained by plotting of Kc/R over $q^2 + kc$ (small squares represent the measured values). By extrapolation of q^2 to zero and c to zero (points are the extrapolated values) R_{g} and A_2 can be determined from the corresponding slope and by the y-intercept we get the molar mass M.

In practice we use Eq. 21 as the following: plotting the measured values $\frac{Kc}{R}$ vs. $q^2 + kc$ (k represents a constant) a typical Zimm plot such as shown in Fig. 9 is obtained. In this example, a solution of four different concentrations (c_1, ..., c_4) was measured at five different scattering angles θ or q. As already mentioned, the detected intensity $I(q)$ is independent of the particle interaction only for very dilute solutions. That is why the lower the concentration that is chosen, the more accurate is the result. In practice, a

series of samples with different concentrations is measured and then these values are extrapolated to $c \to 0$ (see points in the graph). In order to neglect any angular or q-dependence we also fit $q \to 0$. The two following equations belong to the corresponding lines of the extrapolated values.

$$\overset{(21)}{\to} \quad \frac{Kc}{R}(c=0) \; = \; \frac{1}{M}\left(1 + \frac{1}{3}\left\langle R_{\mathrm{g}}^2 \right\rangle q^2\right) \tag{22}$$

$$\overset{(21)}{\to} \quad \frac{Kc}{R}(q=0) \; = \; \frac{1}{M} + 2A_2 c \tag{23}$$

From the respective slopes we obtain the second virial coefficient A_2 and the radius of gyration R_{g}.

So far, only the case of a monodisperse sample has been considered; particles with the same size and shape. However, if, instead of a monodisperse solution, a polydisperse solution is used, the Zimm analysis yields the average of the molar mass:

$$M = \frac{\sum_{\mathrm{i}=1}^{N} N_{\mathrm{i}} M_{\mathrm{i}} M_{\mathrm{i}}}{\sum_{\mathrm{i}=1}^{N} N_{\mathrm{i}} M_{\mathrm{i}}} \tag{24}$$

and the z-average of the squared radius of gyration:

$$\left\langle R_{\mathrm{g}}^2 \right\rangle_z = \frac{\sum_{\mathrm{i}=1}^{N} N_{\mathrm{i}} M_{\mathrm{i}}^2 s_{\mathrm{i}}^2}{\sum_{\mathrm{i}=1}^{N} N_{\mathrm{i}} M_{\mathrm{i}}^2} \tag{25}$$

In this case, the sample consists of N particle species of different molar mass and different size. N_{i} is the number of scattering particles of species i.

Form factor $P(q)$ of a sphere:

The form factor describes the angluar change in the detected intensity due to the intramolecular interference. The scattered intensity changes at different scattering angles q depending on the shape and size of the solute particles. For example, for a homogeneous spherical particle with a radius R the form factor reads:

$$P(q) = \frac{9}{(qR)^6} \left(\sin(qR) - qR\cos(qR) \right)^2 \tag{26}$$

The graph of $P(qR)$ over qR (Eq. 26) is shown in Figure 10.
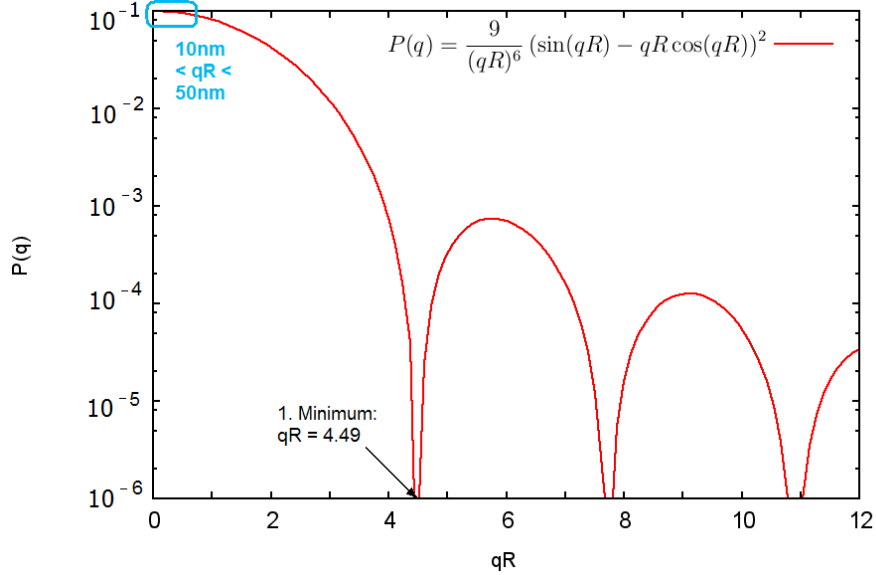
Figure 10: Form factor for a large spherical particle.

The first minimum of $P(qR)$ corresponds to a constant of $qR = 4.49$ which can be used to determine the size of the particles. From Eq. 26, one can see that if a particle with a radius of $R = 15\,\mathrm{nm}$ is examined, the form factor becomes angle independent, qR is always smaller than 0.4, even at $\Theta = 150\,°\mathrm{C}$. As depicted in Figure 10, the form factor is approximately a constant. If the particles have a radius $R = 300\,\mathrm{nm}$, the form factor $P(q)$ shows strong angle dependence. In this case, the values for qR are between 2 and 7.6 considering angles between $30\,°$ and $150\,°$. In practice, measuring such large spherical particles, an oscillating intensity distribution like the one in Figure 10 will be visible. The form factors of spheres with different sizes are shown in Fig. 11:
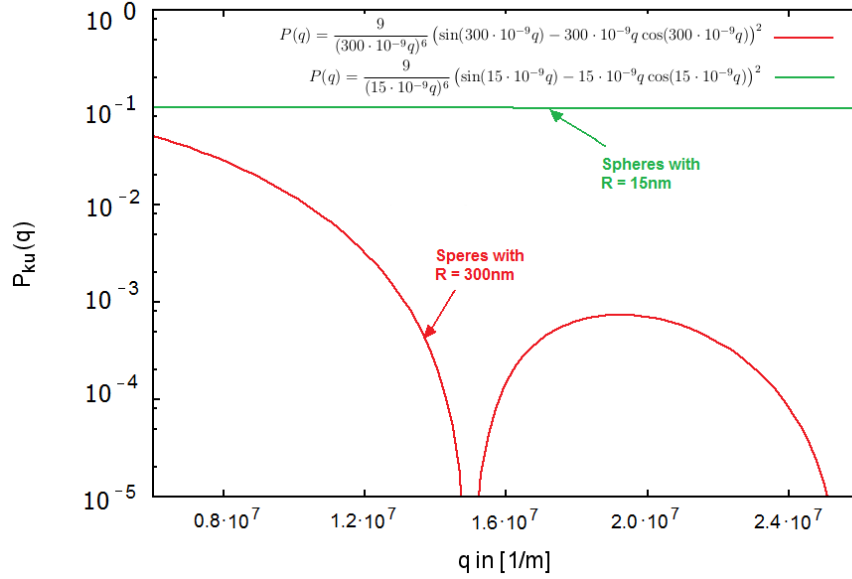
Figure 11: Form factors of spheres with different sizes, $P(q)$ as functions of q.

3.2 Dynamic Light Scattering (DLS)

In the description of the scattering behavior of dissolved particles, the fact that the scattered particles move has been ignored so far. This thermal, continuous and random diffusion is called Brownian motion. This movement is caused by the thermal density fluctuations of the solvent. While for static light scattering the average of the detected intensity is considered, for dynamic light scattering the movement of molecules is important. The basis for this is that intensity fluctuations of the scattered radiation can be observed over time, since the distances between the scattering centers change constantly. This results in a time-variable interference of the scattered light, see Fig. 12.

3.2.1 Time-Intensity-Autocorrelation function

To quantitatively analyze the particle mobility by light scattering, it is helpful to express the scattering intensity fluctuations in terms of a correlation function, as will be discussed in detail in this section. In practice, the scattering intensity $I(t)$ is measured in very small time intervals Δt. Therefore, the time interval Δt should be shorter than the dynamic processes in the solution. The detected intensity is then used by a correlator to calculate the normalized time-intensity-autocorrelation function $g_2(\tau)$. In a measurement of time T_M, this total time can be divided into N discrete measurement intervals Δt, for which:
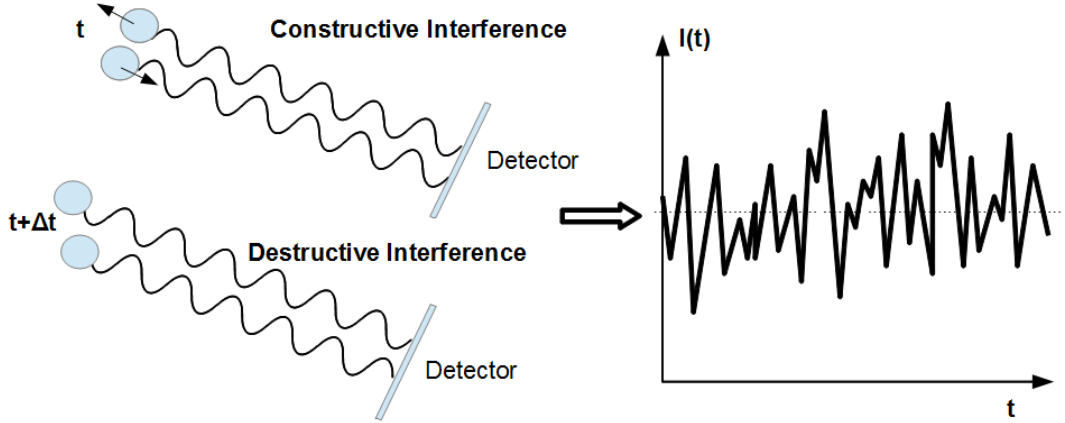
Figure 12: Illustration of how the time-dependent interference can occur. The resulting scattering intensity fluctuates around the average $\langle I \rangle$, which is used for SLS.

$$\tau = n\Delta t \ \text{ with } \ 0 \leq n \leq N \ \text{ and } \ N \cdot \Delta t = T_{\mathrm{M}} \tag{27}$$

Thus τ assumes only integer multiples of Δt. The time-intensity-autocorrelation function can then be expressed as follows:

$$\langle I(t) \cdot I(t+\tau) \rangle \cong \frac{1}{T_{\mathrm{M}}} \sum_{\mathrm{t}=0}^{T_{\mathrm{M}}} I(t) \cdot I(t+\tau) \Delta t \tag{28}$$

In words this means that the time-dependent scattered intensity is multiplied with itself after it has been shifted by a distance τ in time. Therefore, the values have to be summed up. In order to average the sum, it has to be divided by the measurement time T_{M}. The autocorrelation function is then set up for many different delay times τ. The autocorrelation function is not depending on t but only on the delay time τ.

Limits: As pictured in Figure 13, a strong correlation of the molecule movement for small time intervals τ_{small} can be found. $I(t)$ and $I(t+\tau)$ often have the same sign and the product $(I(t) \cdot I(t+\tau))$ is positive, regarding $\langle I(t) \rangle$ as zero level. For $\tau \to 0$ the difference between $I(t)$ and $I(t+\tau)$ diminishes:

$$\lim_{\tau \to 0} \langle I(t) \cdot I(t+\tau) \rangle = \langle I(t)^2 \rangle \tag{29}$$

For large time intervals τ_{large} the movement of the molecules is no longer correlated. Both, positive products as well as negative products occur with the same probability. That is why $\langle I(t) \cdot I(t+\tau) \rangle$ falls off exponentially with increasing τ. The faster the scatterers are moving in the solution, the steeper is the exponential decay of the autocorrelation function. For the limit $\tau \to \infty$ applies:

$$\lim_{\tau \to \infty} \langle I(t) \cdot I(t+\tau) \rangle = \langle I(t) \rangle^2 \tag{30}$$
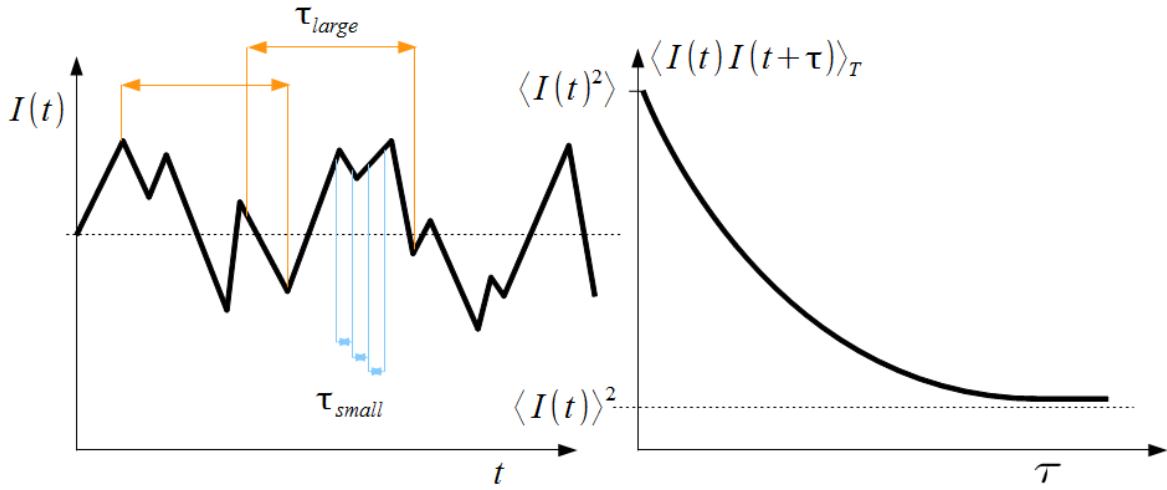
Figure 13: Autocorrelation.

If you choose the time intervals sufficiently small, the sum of Eq. 28 becomes an integral:

$$\langle I(t) \cdot I(t+\tau) \rangle = \frac{1}{T_{\text{M}}} \int_{t=0}^{T_{\text{M}}} I(t) \cdot I(t+\tau) \Delta t \tag{31}$$

To obtain the normalized intensity-time autocorrelation function $g_2(\tau)$, Equation 31 is normalized by $\langle I(t) \rangle^2$:

$$g_2(\tau) = \frac{\langle I(t) \cdot I(t+\tau) \rangle}{\langle I(t) \rangle^2} \tag{32}$$

3.2.2 Siegert relation

Since, in practice, the measured intensity $I(t)$ is proportional to the square of the electric field amplitude $E(t)$ of the scattered light which is directly related to the dynamic behavior of the particles (Brownian motion), for the evaluation of dynamic light scattering, the normalized field temporal autocorrelation function $g_1(\tau)$ is needed:

$$g_1(\tau) = \frac{\langle E(t) \cdot E^*(t+\tau) \rangle}{\langle E(t) E^*(t) \rangle} \tag{33}$$

$g_1(\tau)$ and $g_2(\tau)$ are linked by the Siegert relation:

$$\boxed{g_2(\tau) = 1 + \beta g_1(\tau)^2} \tag{34}$$

The factor β describes an apparatus-dependent constant.
For a monodisperse particle system the field-time-autocorrelation function $g_1(\tau)$ is given by a single exponential with decay rate Γ.

$$\boxed{g_1(\tau) = e^{-\Gamma\tau}} \tag{35}$$

The decay rate Γ is connected to the diffusion coefficient D_s:

$$\Gamma = D_\mathrm{s} \cdot q^2 \tag{36}$$

The diffusion coefficient D_s is related to the hydrodynamic radius R_h of the scattering particles via the Stokes-Einstein-equation:

$$\boxed{D_\mathrm{s} = \frac{k_\mathrm{B}T}{6\pi\eta R_\mathrm{h}}}, \tag{37}$$

In practice, the above-described theory is used as the following: For each measurement a correlator determines the autocorrelation function $\beta g_1(\tau)^2 = g_2(\tau) - 1$ by using a large range of τ from a few ps to several seconds. For each measurement an exponentially

decreasing autocorrelation function is obtained. From the exponential decay rate Γ of these autocorrelation functions the diffusion coefficients $D_{s,i}$ are obtained, from which the hydrodynamic radius R_h can be determined by using the Stokes-Einstein relation.

For poly-disperse samples with n different particles the field-time autocorrelation function is described by a superposition of several exponential functions:

$$g_1(\tau) = \sum_{i=1}^{n} \gamma_i e^{-\Gamma_i t} \tag{38}$$

γ_i is the weight of the individual terms. By Eq. 36 Γ_i and the respective diffusion coefficient $D_{s,i}$ are linked.

4 Experimental Setup

The general structure of a light-scattering apparatus is shown in Fig. 14.
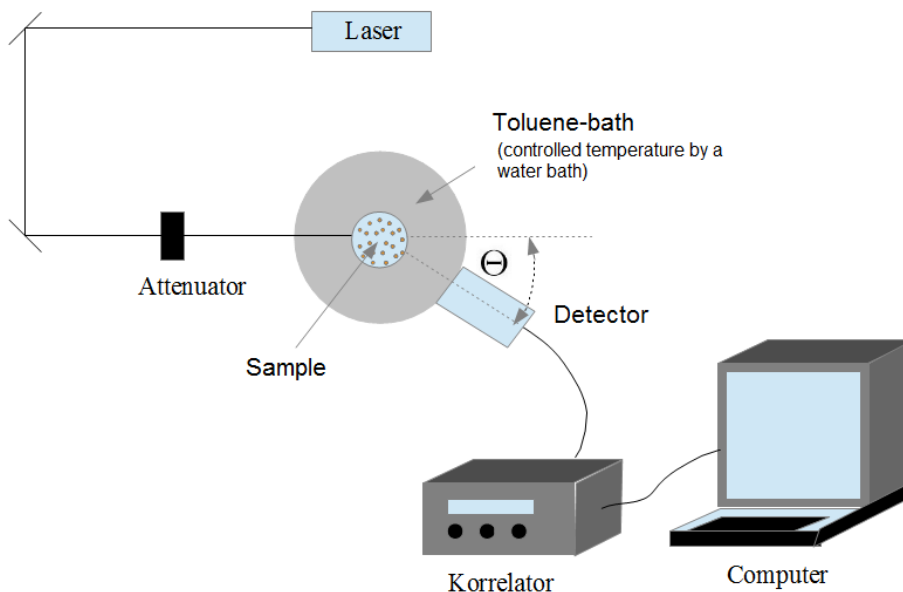
Figure 14: Schematic structure of a light scattering apparatus.

The static and dynamic light scattering experiments will be performed using the *'ALV/CGS-3 compact goniometer system'* (shown in Fig. 15). By using this apparatus both SLS as well as DLS can be performed simultaneously. The instrument is operated using the corresponding computer program *'ALV Correlator Software V.3.0'*. It stores the correlation data as well as the normalized intensity data (compare Chapter 6.1).

The light source is an already vertically polarized helium-neon laser with a known wavelength of $\lambda = 632.8$ nm. The laser produces a coherent and strong intensity light that is directed onto a sample in a toluene bath. The toluene bath is used for temperature regulation of the sample and also to avoid reflections. Toluene is used because the quartz cuvette of the toluene bath and toluene have approximately the same refractive index. In this way disturbing reflections can be minimized.

Dissolved particles scatter light in all directions. In order to detect all of these scattered light waves, the detector is mounted on a goniometer. In this way, scattering angles between $12°$ and $152°$ can be measured. In this experiment angles between $30°$ and $150°$ are used. The correlator processes the registered angle dependent intensity into a normalized field-time-autocorrelation function $g_1(\tau)$. It uses delay times τ from 25 ns up to 3435.9 s. To accommodate the optimal intensity at the detector, the attenuator

determines how much intensity should pass to the detector (pinhole). This helps to prevent damages of the detector due to an excessive input signal.
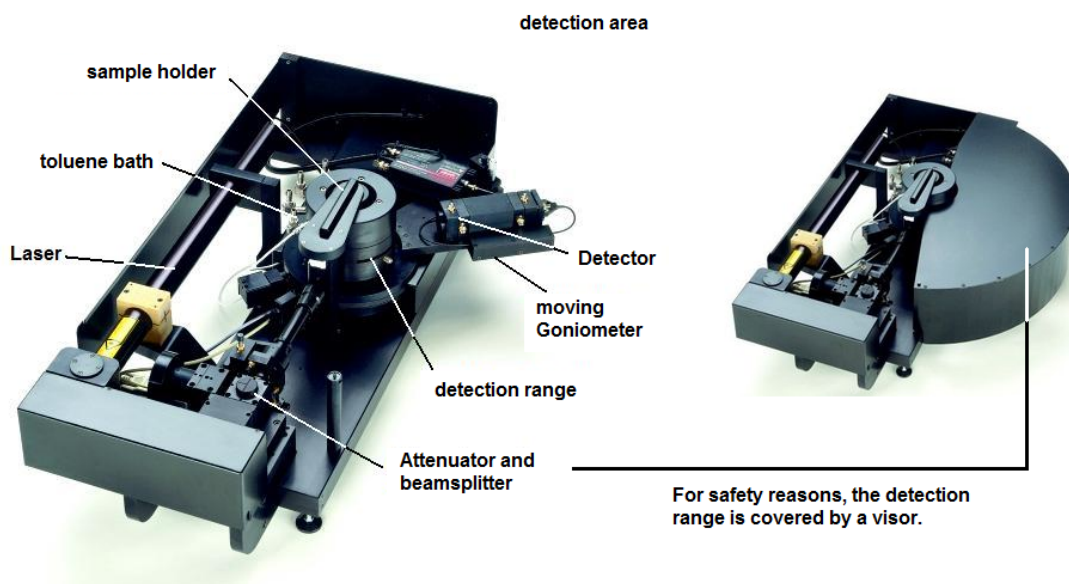

Figure 15: Setup of the 'ALV/CGS-3 Compact Goniometer System'.

5 Experimental Procedure

In this experiment, we will perform standard DLS measurements on two colloidal systems and a protein solution with different sizes:

- Latex beads with a diameter $d = 600\,\mathrm{nm}$ (**LB600**)

- Gold colloid with a diameter $d = 30\,\mathrm{nm}$ (**GC30**)

- A protein sample with a diameter $d \approx 5 - 8\,\mathrm{nm}$ (**Protein**)

The results will be used to determine the angle dependent relaxation time, the diffusion coefficient D_s, and the hydrodynamic radius R_h by using the Stokes-Einstein relation.
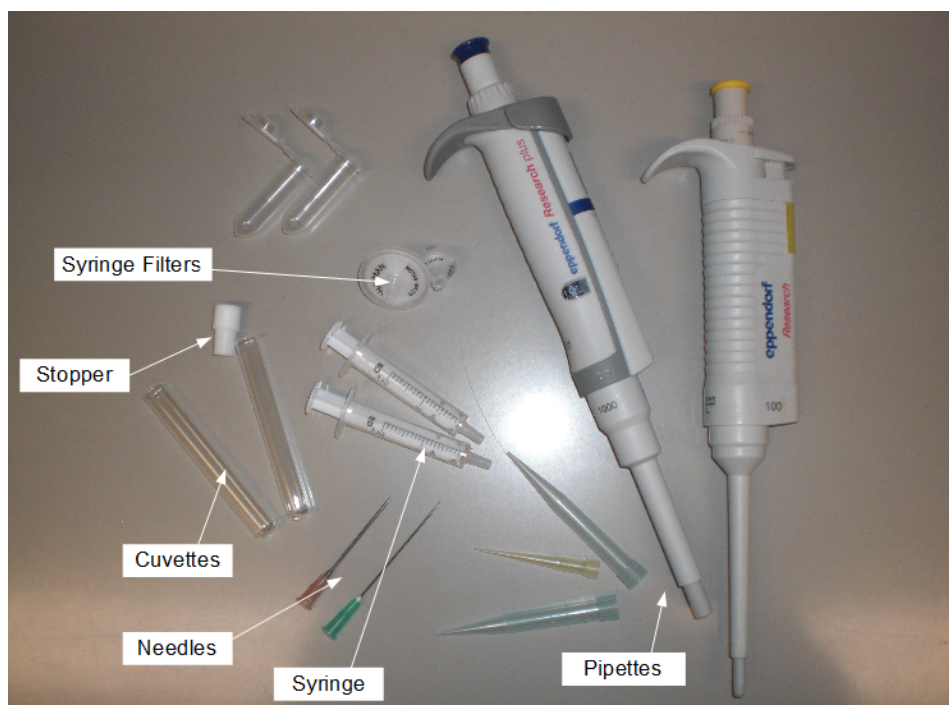
Figure 16: Some important equipment for preparation.

5.1 Sample Preparation

Figure 16 shows most of the equipment you need to prepare the samples.

Preparing the sample you have to pay close attention to avoid dust in the cuvette! Due to their big size of a few µm they scatter light much stronger than the dissolved sample particles whose sizes are in the range of some nm. This leads to large measurement errors.

Start by rinsing the cuvette with acetone to make sure that the cuvette is free of dust. The sample is filtered into the cuvette through a syringe filter (depending on the sample between 0.1 µm and 1.6 µm pore size). Then, the plug has to be set on the cuvette as soon as possible. (A more detailed instruction on sample preparation, such as the use of pipettes, are given on the day of the experiment by the assistant.)

5.2 Measurement 1: Latex beads with a diameter of 600 nm (LB600)

Prepare the LB600 solution from a stock solution whihc has been 100.000-fold diluted. Fill about 1.5 ml stock solution into a syringe and filter it with a 1.6 µm filter into a already cleaned cuvette. After filling the cuvette with the sample, it has to be rinsed

with acetone on the outside to keep the toluene bath of the apparatus clean. Afterwards, the cuvette has to be put into the sample holder of the instrument.

Meanwhile, choose *'General DLS and SLS'* from the menu bar to set that you want to do a 'standard' measurement:
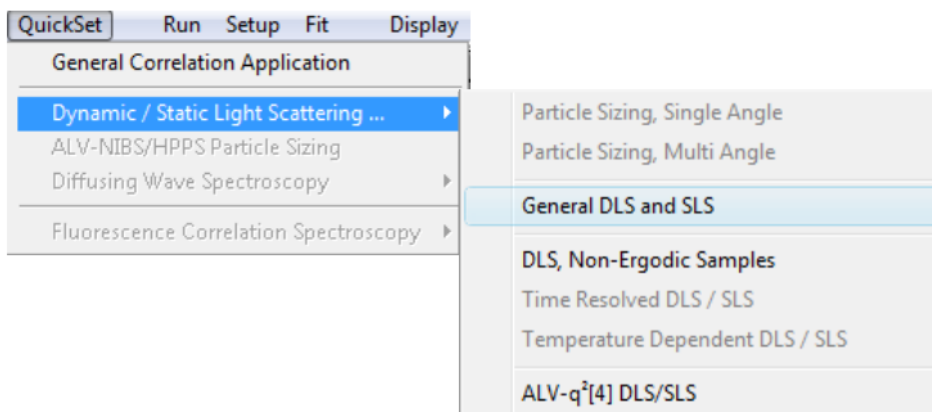
The main window will be opened which allows you to control the apparatus (see Fig. 17). Basically all of the settings for the measurement have to be done here further information can be found on the right side of the graphic.
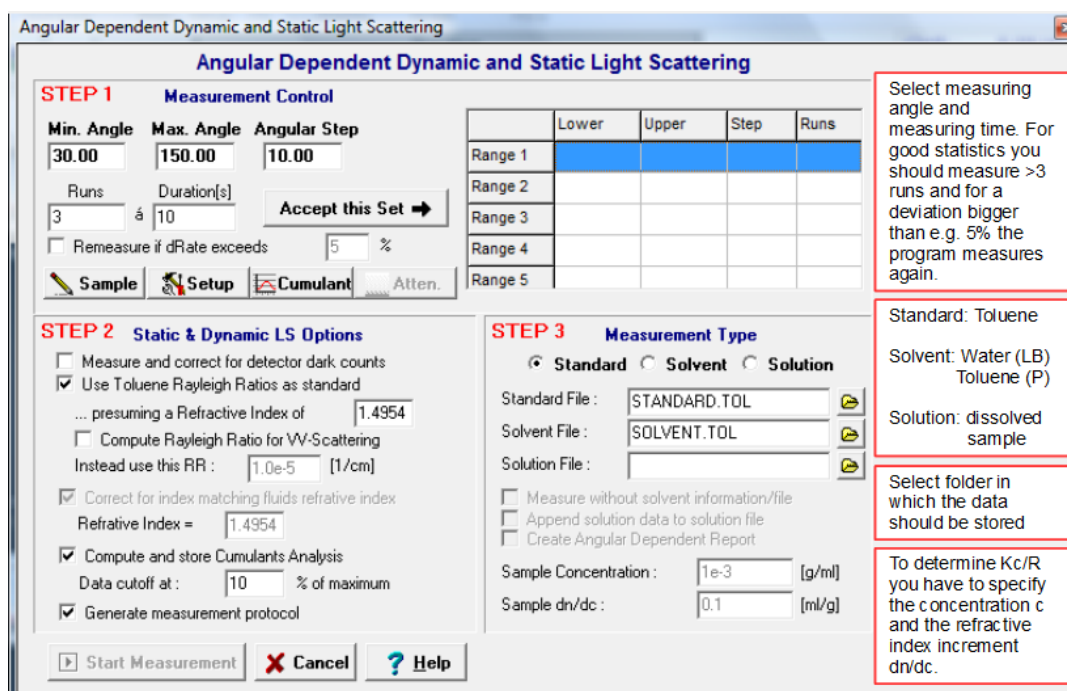
Figure 17: Control of light scattering apparatus.

Caution: Before starting the measurement of the sample, make sure that the button 'Solution' is marked in STEP 3! Otherwise, the standard or the solvent file will be overwritten and the measurement will have to be started once again!

To choose where to store your data, click 'File' → 'Set AutoSave'. The window shown in Fig. 18 opens. Accept to automatically save the data. Select the storage 'e:data' and the folder of your group, which has been created previously. Finally, rename the measurement (here, for example: LB600). This setting has to be done before each measurement to ensure that the location and the stored name can be changed.
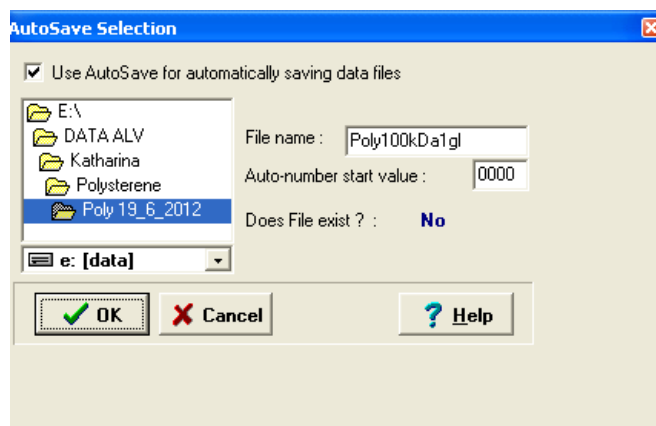
Figure 18: Autosave

Afterwards, Open the window shown in Fig.17 and choose in STEP3 'Solution'. The folder has to be selected as well, in which you want to store the data. Enter the same file name that you have previously registered in the 'Auto Save' settings.

Start the measurement with the following suggested setting parameters:

- <u>Measurement:</u> 3 times 30 s

- <u>Angle:</u> from 30° to 150° with a step of 2.5°

- No darkcount, error 10 percent

5.3 Measurement 2: Gold Colloids with a diameter of 30 nm (GC30)

Take about 1 ml gold colloid solution and filter it with a 0.1 μm filter into the clean cuvette. Start the measurement with the following suggested setting parameters:

- Measurement: 3 times 30 s

- Angle: from 30 ° to 150 ° with a step of 10 °

- No darkcount, error 5 percent

Note: for this step, the supervisor can choose a gold colloid solution with unknown size for the measurement.

5.4 Measurement 3: Proteins in solution

A protein solution will be prepared and filtered with a 0.1 µm filter into the clean cuvette. The protein solution should contain 10 mg/ml bovine serum albumin (BSA) with 0.1 mM NaCl prepared from stock solutions. Start the measurement with the following suggested setting parameters:

- Measurement: 3 time 30 s

- Angle: from 30 ° to 150 ° with step of 10 °

- No darkcount, error 5 percent

6 Data Analysis

6.1 Stored data

DLS-Data:
By the autosave-setting (see Fig. 18), all the measurements from the correlator are automatically stored in text files. For each angle three runs are measured. At the end, there are four auto-correlation-functions, three for each measurement and one averaged one. For the evaluation we use the averaged text files. In figure 19 it is shown how the correlation files are stored. All important information is contained in these text files. The following values can be found in the files: temperature T, viscosity η, refractive index n, measuring angle θ and more. The values for the determination of the diffusion coefficient can be found in the columns and rows labeled 'Correlation' (see Fig. 19). The first column corresponds to the delay time τ and the second one to the normalized intensity-time autocorrelation function $g_2(\tau) - 1$. Plotting $g_2(\tau) - 1$ over q^2, we obtain the exponential function, which can be seen during the measurements in the upper left. Beyond these values there are much more table columns with e.g. the count rate and

other data which are not relevant for our evaluation.
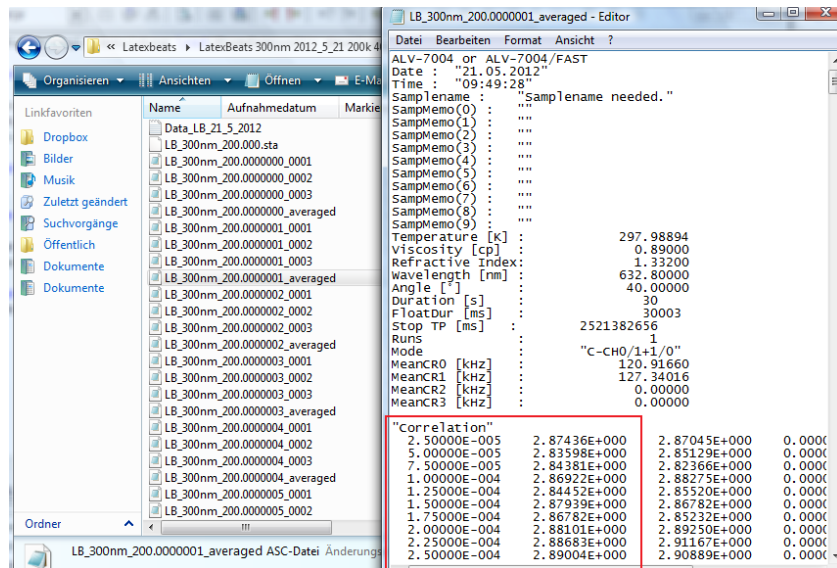
Figure 19: Files stored (left) and open text file with all the information (right) - DLS analysis.

<u>**SLS-Data**</u>:

The value $\frac{Kc}{R}$ can be taken directly from the measurement. After each measurement, or after each measured angle $\frac{Kc}{R}$ is displayed directly on the screen in a table (see Fig. 20). When the measurement is finished, the data has to be copied and stored separately in a text file! It is important to remember this after each measurement, because otherwise it is very difficult to re-check the data!

6.2 Analysis methods of the DLS data

1. CONTIN-Algorithm:

The correlation function $g_1(\tau)$ can be evaluated in different ways. Directly during the experimental procedure, it is possible to calculate the radius of the dissolved particles by using the CONTIN algorithm. This analysis of the correlation function is based on an inverse Laplace transform. This gives the plot as shown in Fig. 20 on the lower right side. For monodisperse samples only one peak (Fig. 21) can be seen. On the x-axis you find the radius of the dissolved particles. For polydisperse samples, depending on the number of different particles, several peaks can be seen:

2. Second analysis method:
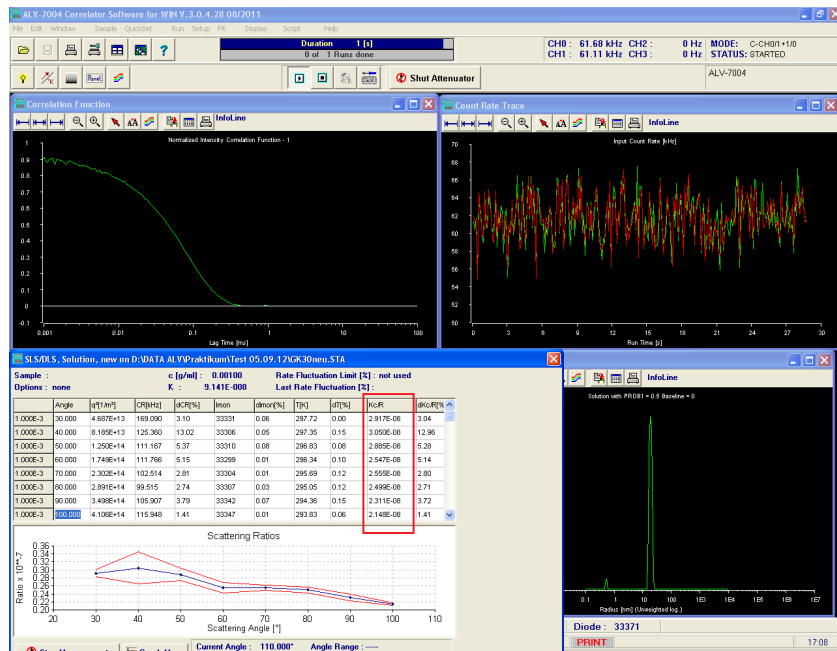
Figure 20: Screenshot during the measurement. Intensity fluctuations (top right), particle size (bottom right) determined by the CONTIN-algorithm that uses the values of the correlation (top left). The measured $\frac{Kc}{R}$-values at each angle are shown in the table and are used for the SLS evaluation.
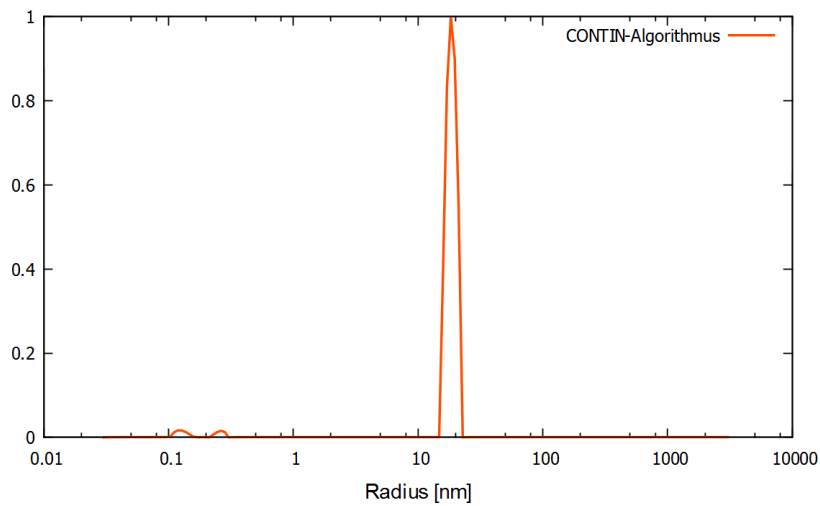

Figure 21: In the editor stored CONTIN-data plotted with Gnuplot. In this example you find particles with a radius of $R \approx 15\,\text{nm}$.

The 'common' method to evaluate the autocorrelation function works as follows:

Monodisperse sample: The (correlation-)data from Figure 19 correspond to the intensity-time autocorrelationfunction $g_2(\tau) - 1$. Therefore Eq. 35 fits to the experimentally determined data.

$$g_2(\tau) - 1 = \beta \cdot g_1(\tau)^2 = \beta \cdot e^{-2\Gamma\tau} \tag{39}$$

β describes an apparatus-dependent constant. Taking the square of Equation 35 and considering Equation 36 leads to: $-2\Gamma = 2D_s q^2$. In this way, for each angle one Γ is obtained. To determine the averaged diffusion coefficient D_s , Γ vs. q^2 has to be plotted. If the dissolved particles are small, a linear dependence between Γ and q^2 prevails. The slope of this fit gives the diffusion coefficient $2D_s$. **Note the factor 2 for further analysis!** This diffusion coefficient is used to determine the hydrodynamic radius R_h using the Stokes-Einstein equation (37).

6.3 Analysis measurement 1: Latex beads (LB600)

For this measurement, we mainly focus on the static light scattering by describing the form factor $P(q)$ of LB600.
From Equation 21 the following proportionality is obtained:

$$P(q) \propto \frac{R}{Kc} \tag{40}$$

Plot the measured ratio $\frac{R}{Kc}$ over q and compare it to the theoretical curve from Eq. 26. There is no need to fit $P(q)_{\text{theo}}$ to the measured data, only adjust the theoretical curve to the measured one by iteratively varying the radius R and by multiplying by a prefactor $\alpha \cdot P(q)_{\text{theo}}$. The theoretical curve is not obliged though. Plot $\frac{R}{Kc}$ for all three different samples in one figure to identify their angular dependent scattering. The final image should look similar to Figure 11.
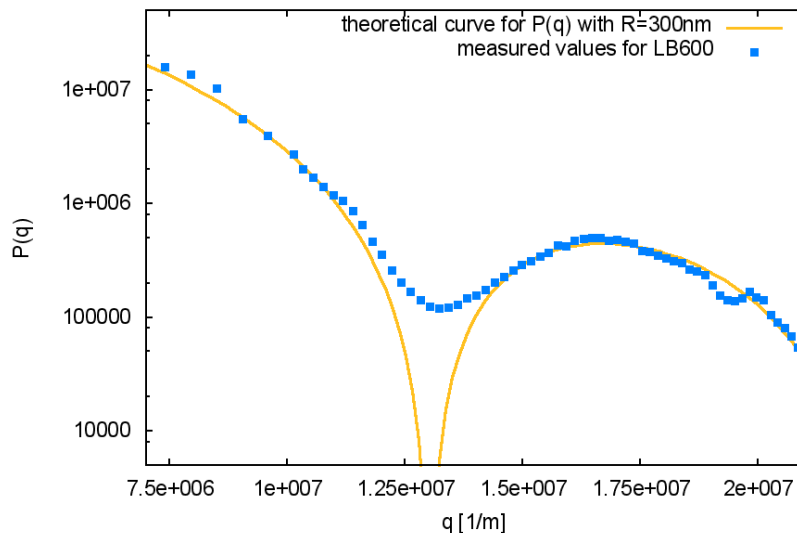
Figure 22: Example plot of the form factor of LB600 with experimentally determined intensity (solid circles) and the theoretical model for monodisperese spheres (solid line). In this example the particles have a radius of $R \approx 300\,\mathrm{nm}$.

6.4 Analysis measurement 2: Gold colloids (GC30) and proteins

Same method applies to the analysis of LB600 and protein sample

For this measurement, we focus on the diffusion coefficient D_s and the hydrodynamic radius R_h from the dynamic light scattering results. However, the similar analysis (SLS data) as has been done for LB600, could be performed as well.

The DLS measurement has been performed from 30° to 150° in 10°-steps. For this measurement, we will analyze the dynamic data to get the diffusion coefficient of the gold colloid. First, determine the values of Γ for each angle by fitting the data using Eq. 39. An example is shown in Fig. 23.

Second, plot Γ vs. q^2. For small scattering vectors q^2 the values increase linearly. For the linear part it is necessary to make a linear regression.

In the protocol, the graph of Γ vs. q^2 has to be attached. The chart should also include the linear fit. Write down the equation of the regression. From the diffusion coefficient D_s one can calculate the hydrodynamic radius R_h by using the Stokes-Einstein relation. An example is shown in Fig. 24.
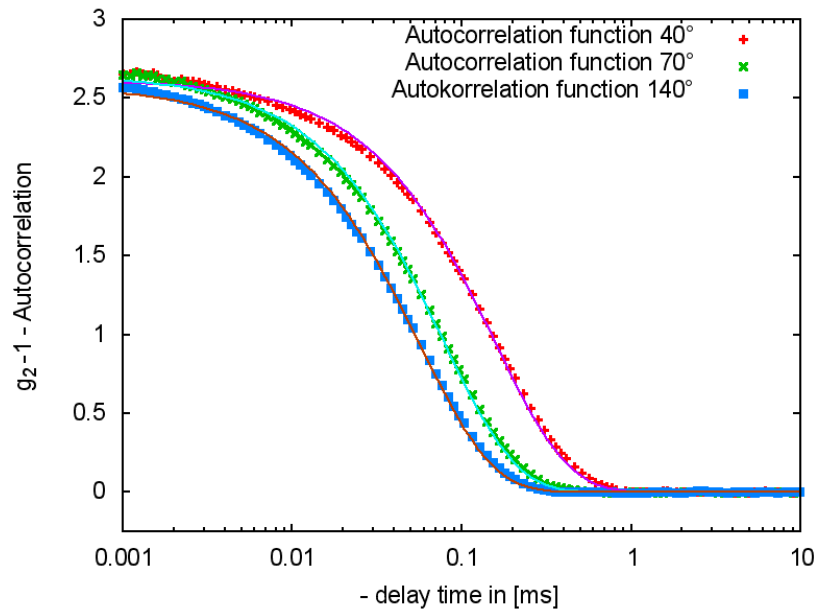
Figure 23: Example plots of the intensity-time autocorrelation function $g_2(\tau) - 1$ with data fitting using Eq. 39.
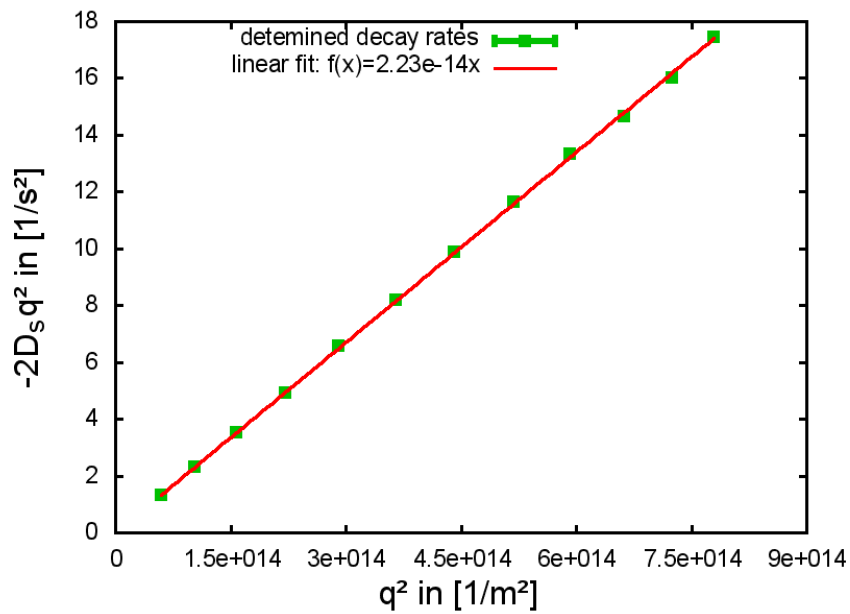

Figure 24: Example plot of Γ vs. q^2 and a linear fitting. From the slope one obtains the diffusion coefficient D_{s}.

Table with a few important constants

solvent	$\eta(20°C)$	$n(20°C)$
Toluene	0.59	1.496
Water	1.00	1.332

Table 1: Properties of the solvents (viscosity η and refractive index n (data from Sigma Aldrich).

7 Instruction for Report Preparation

Please bring with you a USB stick at the day of the experiment!

The goal of this experiment is to understand the basic principles of the scattering technique and its application to nano-, bio- and other soft matter systems. After performing the experiment, a short report is needed to summarize this lab course. In general, the following items should be included:

Basic Principles of Light Scattering

Try to summarize the basic principles we introduced for dynamic light scattering by answering and explaining the following questions:

- How is the scattering vector $\vec{q}$ defined?

- For dynamic light scattering, could you summarize the basics on how to determine the diffusion coefficient from the time correlation function of scattering intensity via the Siegert relation?

- Which equation allows to obtain the hydrodynamic radius R_h from the diffusion coefficient?

Experimental setup and experimental procedure

Briefly describe what the experimental setup looks like; what are the basic components? Describe which samples have been measured on the day of the experiment. Describe the exact details of the experiment, such as angle range and increment, duration, error, etc. Please describe the procedure of checking the scattering speckles using laser pointers. Attach one or two pictures you took during the experiments. Please describe what you see and give a possible reason.

Data Analysis

This is the major part of the report. You may wonder what to do with the huge amount of data collected during the experiment. The section of Data Analysis has provided detailed description on how to do all the data analysis. However, in the report, it is not necessary to do all data analysis. Basic requirement is described below:

- For static data of three samples, please plot the measured ratio $\frac{R}{Kc}$ over q in logarithmic scale and compare their angle dependent scattering.

- For GC30, please show a few angles (e.g 90°) of the time correlation function. Plot the intensity $g_2(\tau) - 1$ vs. τ, then fit the data using Eq. 38. If you repeat the above analysis for all angles and plot Γ vs. q^2, one should obtain a linear relationship. A simple linear fit will give you the value of the diffusion coefficient D_s. You can further calculate the hydrodynamic radius R_h using the Stokes-Einstein relation.

- Apply the above analysis for LB600 (use only the first 10 data for better statistics) and protein samples. Summarize and compare the results for samples with different sizes.

- Summarize your results for the hydrodynamic radii and the diffusion coefficients for your different samples in a table like the following.

sample	LB600	GC	Protein
D_s [cm^2/s]			
R_h [nm]			

- For those who are interested in further data analysis, please check the whole procedure in the section of Data Analysis.

Suggestion for further improvement

Any comment for further improvement of the practical is welcome!

8 Bibliography

1. W. Schärtl, Light Scattering from Polymer Solutions and Nanoparticle Dispersions, Springer Verlag 2007

2. P. N. Pusey, Dynamic Light Scattering, in Neutrons, X-ray and Light: Scattering Methods Applied to Soft Condensed Matter. 2002, Ed. P. Lindner, T. Zemb, Elsevier Sicence, Amsterdam.

3. Bruce J. Berne, Robert Pecora, Dynamic Light Scattering - With Applications to Chemistry, Biology, and Physics http://www.uni-regensburg.de/Fakultaeten/nat _Fak_IV/Physikalische_Chemie/Kunz/student/Versuche/Licht

4. Praktikumsanleitung Universität Köln: http://www.meerholz.uni-koeln.de/fileadmin/user_upload/Docs/Praktikum/ Versuchsanleitungen/Skript-Lichtstreuung_A._Mueller.pdf